TISSUE ENGINEERING: Part A
Volume 19, Numbers 3 and 4, 2013

DOI: 10.1089/ten.tea.2012.0158

Pro-angiogenic and Anti-inflammatory Regulation by Functional Peptides Loaded in Polymeric Implants for Soft Tissue Regeneration

Angela L. Zachman, MS,[1,2] Spencer W. Crowder, MS,[1,2] Ophir Ortiz, PhD,[3] Katarzyna J. Zienkiewicz, MS,[1] Christine M. Bronikowski,[1] Shann S. Yu, MS,[1] Todd D. Giorgio, PhD,[1,4] Scott A. Guelcher, PhD,[1,2,4] Joachim Kohn, PhD,[3] and Hak-Joon Sung, PhD[1,2]

Inflammation and angiogenesis are inevitable *in vivo* responses to biomaterial implants. Continuous progress has been made in biomaterial design to improve tissue interactions with an implant by either reducing inflammation or promoting angiogenesis. However, it has become increasingly clear that the physiological processes of inflammation and angiogenesis are interconnected through various molecular mechanisms. Hence, there is an unmet need for engineering functional tissues by simultaneous activation of pro-angiogenic and anti-inflammatory responses to biomaterial implants. In this work, the modulus and fibrinogen adsorption of porous scaffolds were tuned to meet the requirements (i.e., ~100 kPa and ~10 nm, respectively), for soft tissue regeneration by employing tyrosine-derived combinatorial polymers with polyethylene glycol crosslinkers. Two types of functional peptides (i.e., pro-angiogenic laminin-derived C16 and anti-inflammatory thymosin β4-derived Ac-SDKP) were loaded in porous scaffolds through collagen gel embedding so that peptides were released in a controlled fashion, mimicking degradation of the extracellular matrix. The results from (1) *in vitro* coculture of human umbilical vein endothelial cells and human blood-derived macrophages and (2) *in vivo* subcutaneous implantation revealed the directly proportional relationship between angiogenic activities (i.e., tubulogenesis and perfusion capacity) and inflammatory activities (i.e., phagocytosis and F4/80 expression) upon treatment with either type of peptide. Interestingly, cotreatment with both types of peptides upregulated the angiogenic responses, while downregulating the inflammatory responses. Also, anti-inflammatory Ac-SDKP peptides reduced production of pro-inflammatory cytokines (i.e., interleukin [IL]-1β, IL-6, IL-8, and tumor necrosis factor alpha) even when treated in combination with pro-angiogenic C16 peptides. In addition to independent regulation of angiogenesis and inflammation, this study suggests a promising approach to improve soft tissue regeneration (e.g., blood vessel and heart muscle) when inflammatory diseases (e.g., ischemic tissue fibrosis and atherosclerosis) limit the regeneration process.

Introduction

Biomedical implants are often rendered ineffective due to inflammatory responses, such as fibrous capsule formation.[1–4] Activated macrophages aid in host defense by producing reactive oxygen species and cytokines, including interleukin-1β (IL-1β), IL-6, IL-8, and tumor necrosis factor alpha (TNF-α).[5–7] For successful integration of implants, it is ideal to have the device surrounded and penetrated by highly vascularized tissue.[8] During angiogenesis, the vascular endothelium undergoes morphological and functional changes that are stimulated by inflammatory mediators, including vasodilation and increased capillary permeability.[9,10] On the other hand, inflammation is exacerbated by the activation of angiogenesis.[11,12] These examples demonstrate that inflammation and angiogenesis are intrinsically linked and challenging to decouple,[13–18] indicating an unmet need for successful tissue regeneration through independent control of angiogenic and inflammatory responses to biomaterial scaffolds.

The goal of this study is to develop a means by which pro-angiogenic and anti-inflammatory responses to implanted

[1]Department of Biomedical Engineering, Vanderbilt University, Nashville, Tennessee.
[2]Center for Matrix Biology, Vanderbilt University Medical Center, Nashville, Tennessee.
[3]New Jersey Center for Biomaterials, Rutgers University, Piscataway, New Jersey.
[4]Department of Chemical and Biomolecular Engineering, Vanderbilt University, Nashville, Tennessee.

Table 1. Sequence and Function of Peptides

Type	*Activity*	*Origin*	*Sequence*
C16	Pro-angiogenic	Laminin-1	Lysine-Alanine-Phenylalanine-Aspartic acid-Isoleucine-Threonine-Tyrosine-Valine-Arginine-Leucine-Lysine-Phenylalanine
Ac-SDKP	Anti-inflammatory	Thymosin β-4	N-acetyl-serine-Aspartic acid-lysine-proline

biomaterials can be activated simultaneously for regeneration of soft tissues (e.g., blood vessel and cardiac muscle), in particular, when the regeneration process is hampered by inflammatory diseases (e.g., ischemic tissue fibrosis and atherosclerosis).[19–22] To alter the modulus and fibrinogen adsorption of porous scaffolds, tyrosine-derived combinatorial polymers[23,24] were crosslinked with polyethylene glycol (PEG) dihydrazides,[25] and fabricated into porous scaffolds by salt leaching. Pro-angiogenic and/or anti-inflammatory responses were activated by embedding functional peptides (Table 1) within the collagen gel into the pores of scaffolds. Laminin-1-derived pro-angiogenic C16 peptides promote endothelial cell (EC) adhesion, tube formation, and angiogenesis.[26,27] Thymosin β-4-derived anti-inflammatory Ac-SDKP peptides have been identified to decrease macrophage infiltration and TGF-β expression.[19,20,28,29] Lipopolysaccharide (LPS) was used as a pro-inflammatory control. Angiogenic (i.e., migration, tubulogenesis, and perfusion capacity) and inflammatory responses (i.e., phagocytosis, cytokine production, and F/80 expression) were investigated through a series of *in vitro* mono-/coculture and *in vivo* implantation experiments.

Materials and Methods

Fabrication and characterization of scaffolds

Porous scaffolds. Copolymers of x mole % desaminotyrosyl tyrosine ethyl ester (DTE) and y mole % desaminotyrosyl-tyrosine (DT) were identified as poly(x% DTE-co-y% DT carbonate) and crosslinked with z mole % PEG (Mw = 2000) dihydrazide as previously described.[25] In this study, poly(90% DTE-co-10% DT carbonate) with varying degrees of crosslinking was used because this polymer has been identified to be effective for promoting angiogenesis in a previous study (Fig. 1A).[25] Pores were generated in scaffolds by salt leaching as reported previously.[25] The pore structure and interconnectivity were visualized by imaging with a Hitachi S-4200 scanning electron microscope (SEM) and optical coherence tomography (OCT) (Bioptigen), respectively.

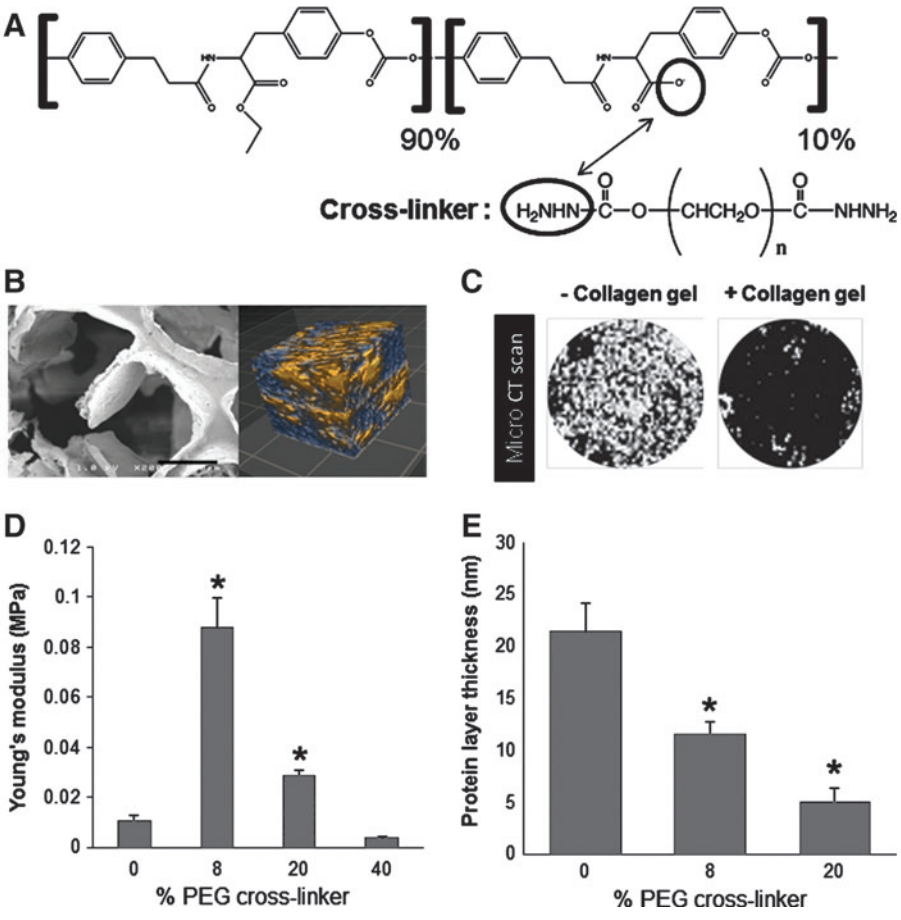

FIG. 1. Scaffold characterization. **(A)** Chemical structure of backbone polymer and polyethylene glycol (PEG) dihydrazide crosslinkers. **(B)** Left: scanning electron microscopy image of pore architecture in a scaffold. Scale bar: 150 μm. Right: optical coherence tomography image of pore interconnectivity (2-×2-×2-mm scan), indicating a highly porous structure with a high degree of pore interconnectivity. Blue, pores; yellow, scaffold. **(C)** Microcomputed tomography scan images showing the entire surface of the scaffold (diameter = 0.6 cm) without (left) and with (right) collagen gel at 7 days after gelation, proving the stability of collagen gel in the scaffold. White area, pores; black area, collagen gel or biomaterial scaffold. **(D)** Young's modulus obtained from compression testing of wet, collagen-filled scaffolds. **(E)** Protein adsorption on scaffolds, as measured by the thickness of adsorbed fibrinogen layer measured using quartz crystal microbalance with dissipation (QCM-D). **(D, E)** *$p < 0.05$ versus 0% PEG crosslinker ($n = 3$). Color images available online at www.liebertpub.com/tea

Peptide loading. Functional molecules (i.e., pro-angiogenic C16, anti-inflammatory Ac-SDKP, and pro-inflammatory LPS) (Table 1) were incorporated into the scaffolds by filling the pores with collagen gel (3 mg/mL; Advance Biomatrix) containing peptides.[19,27,28,30] All peptides were obtained from GenScript. To evaluate the stability of the scaffold–collagen gel association, scaffolds were filled with collagen solution and imaged before and 7 days postcollagen gel formation with a variable geometry Skyscan 1172 Microtomograph (microcomputed tomography [micro-CT]) unit with a 10W X-ray (45 kV) source (Micro Photonics, Inc.).

Mechanical testing. Scaffolds were crosslinked with 0, 8, 20, or 40 molar % PEG dihydrazide and the collagen gel was poured onto the scaffolds, filling the pores. Scaffolds were incubated in water for 2 h before the wet modulus was measured in a submersion chamber using an Instron (Model 5D Materials Testing Machine). The specimens were compressed at a crosshead speed of 0.5 mm/min and the stress vs. strain curve was recorded. The modulus was calculated as the slope of the linear portion of the stress–strain curve ($n = 3$).

Protein adsorption. Gold quartz crystals (QSX 301; Q-Sense) were spin-coated with a mixture 1% weight/volume of backbone polymer and PEG dihydrazide (0%, 8% or 20%) in tetrahydrofuran as described previously.[31] Phosphate-buffered saline (PBS) was first flowed through each chamber to equilibrate, and fibrinogen (3 mg/mL; Sigma Aldrich) in PBS was then run at a flow rate of 24.2 μL/min for 2 h. Fibrinogen was chosen because this plasma protein is prevalent around an injury site.[32,33] A PBS rinse was performed for 1 h to remove any reversibly adsorbed proteins. The Voigt model in Q-Tools (Q-Sense; Biolin Scientific) was used to model overtones 3–9, to obtain the adsorbed protein mass ($\mu g/cm^2$) ($n = 3$) using the previously described methods.[34,35]

Peptide release from scaffolds

Scaffolds filled with a mixture of collagen and either Ac-SDKP or C16 peptides, or the combination of both peptides (75 μg each peptide) were incubated in PBS at 37°C. At each time point of 1, 3, 7, or 14 days ($n = 4$), the amount of peptides in the collected supernatant was detected by high-performance liquid chromatography (HPLC) (Xterra® RP18 column; Waters Corporation) with a flow rate of 0.1 mL/min at 37°C and 220 nm detection wavelength ($n = 4$). A gradient was created starting with 100% mobile phase A (0.1% trifluoroacetic acid [TFA] in water for Ac-SDKP, pure water for C16) for 2 min and gradually changing to 95% mobile phase B (90% methanol with 0.1% TFA in water) over 15 min. This final composition was held for 1 min and increased to 100% mobile phase B after 1 additional minute. The amount of released peptide was calculated based on a standard curve ranging from 0 to 75 μg/mL using the Breeze™ software (Waters).

Cell culture on scaffolds for in vitro *cell assays*

Human umbilical vein endothelial cells (HUVECs) were purchased from Cell Applications and cultured in MesoEndo Endothelial Cell Media (Cell Applications).[36] Human blood-derived monocytes were purchased from Advanced Biotechnologies and differentiated into monocyte-derived macrophages (MDMs) by seeding at a density of 2×10^7 cells/10 mL DMEM (Invitrogen) with 20% fetal calf serum (Intergen), 10% human serum (Nabi), and 5 ng/mL macrophage colony-stimulating factor (Sigma) for 9 days.[37] HUVECs and MDMs were used because they are well-studied models of angiogenesis and inflammation in the tissue remodeling phase, respectively.[36,37] Porous scaffolds with 8% crosslinking were punched into 24-well size discs, sterilized under UV for 1 h per side, and filled with the collagen gel either with or without peptides.

In vitro *angiogenic and inflammatory assays with single cell types*

HUVEC migration. HUVECs (2×10^5 cells/mL media, 1 mL media/scaffold) were labeled with Hoechst 33258 nuclear stain (Sigma) and seeded onto the top surface of collagen-filled scaffolds with or without C16 peptide (75 μg). HUVEC migration from the gel surface into the scaffold pores was imaged at 0 and 72 h(s) postseeding using optical sectioning (3-μm intervals) with a Leica TCS SP2 multiphoton microscope system (Wetzlar). The number of migrated cells, as well as the number of cells remaining on the surface, were counted using ImageJ (National Institutes of Health), and the ratio of migrating to nonmigrating cells was determined ($n = 5$). Proliferating cells were quantified by BrdU incorporation according to the manufacturer's protocol (Millipore).

Tubulogenesis. HUVECs (2×10^5 cells/mL media, 1 mL media/scaffold) were cultured for 72 h on collagen-filled scaffolds with C16 peptide (0, 25, 50, or 75 μg). The maximum amount of peptides (75 μg) was used following the results from the previous studies.[30,38] Cells were fixed with 2% paraformaldehyde in PBS and stained with ethidium bromide nuclear stain (Invitrogen). Cells were imaged at 40 μm into the scaffold with a multiphoton confocal microscope (Leica TCS SP2) and tube length, as measured by drawing lines over elongated cord-like structures of cell–cell interactive HUVECs in three-dimensional (3D), was measured using Microsuite software (AnalySIS; Olympus) ($n = 5$).[25]

Phagocytosis. MDMs (1×10^5 cells/mL media, 1 mL media/scaffold) were cultured for 72 h on collagen-filled scaffolds in the presence of either pro-inflammatory LPS (100 ng) or anti-inflammatory Ac-SDKP peptide (0, 25, 50, or 75 μg). Cells were treated with green fluorescent *Escherichia coli* particles for 2 h according to the manufacturer's protocol (Vybrant® Phagocytosis assay kit; Invitrogen), counterstained with Hoechst, and imaged with a confocal microscope (Leica TCS SP2).[39,40] The green fluorescence intensity was measured and normalized to the corresponding cell number using ImageJ ($n = 5$).

Coculture of MDMs and HUVECs

MDMs (1×10^5 cells/scaffold) were mixed with collagen, cell culture media, and peptides (75 μg) or LPS (100 ng), and this complex was poured into a scaffold and incubated for 2–3 h at 37°C to allow for gelation. HUVECs (2×10^5 cells/mL media, 1 mL media/scaffold) were seeded on top of the scaffold in a 50:50 mixture of MDM culture media and

HUVEC culture media. After 72 h, MDMs were analyzed for phagocytic activity using the Vybrant Phagocytosis assay kit as described above. Samples were fixed and stained for the vascular cell adhesion molecule-1 (VCAM-1: a marker of ECs) using the allophycocyanin-conjugated anti-human CD106 antibody (BioLegend).[41] Cells were counterstained with Hoechst and counted. Tubulogenesis was defined as any three or more VCAM-1-expressing cells joined to form a tube, similar to other studies that monitored tubulogensis in 3D.[42,43] Only VCAM-1-positive HUVECs were of interest in the coculture model because this specifically identified inflammatory-activated HUVECs as opposed to labeling all HUVECs with a ubiquitous EC marker. Cells in the test scaffolds were imaged with an Olympus FV 1000 confocal microscope, and images were analyzed for tubulogenesis (i.e., the number of tubes formed) and phagocytic activity (i.e., fluorescence intensity) ($n = 8$).

Pro-inflammatory macrophage cytokine secretion

MDMs and HUVECs were cocultured following the above protocol. Media samples (12.5 μL/sample) were collected and analyzed for the released amount of pro-inflammatory cytokines (i.e., IL-1β, IL-8, IL-6, and TNF-α) using BD Human Inflammation Cytometric Bead Array and a fluorescence-activated cell sorting Calibur flow cytometer (BD Biosciences) according to the supplier's protocol ($n = 4$).[44]

In vivo *angiogenesis and inflammatory activation in implanted collagen-filled scaffolds*

The Institutional Animal Care and Use Committee (IACUC) at the Vanderbilt University approved all surgical procedures involving animals. Collagen-filled scaffolds containing LPS (100 ng) or peptides (0 or 75 μg) were sandwiched between two nitrocellulose filters with 0.22-μm pore size (Millipore) to constrain nonspecific tissue ingrowth into the scaffolds.[17] Cell-free scaffolds were implanted subcutaneously into the dorsal regions of 129/SvEv mice for 7 days, as an immunocompetent model.[45] Expression of F4/80 membrane-bound antigens on inflammatory cells infiltrated into implants was detected by immunohistochemistry of frozen sections (4% paraformaldehyde fixed, 4-μm sections) from the harvested scaffolds using Alexa Fluor 594-conjugated rat anti-mouse F4/80 monoclonal antibodies (Abcam).[46] The fluorescence intensity was measured and normalized to the corresponding total cell number, identified by Hoechst nuclear stain ($n = 4$). To determine angiogenic and inflammatory activities, fluorescence microangiography and phagocytosis assay were performed. Briefly, heparinized saline (10 mL) containing 0.1 μm fluorospheres (Invitrogen) was perfused into vasculature through injection into the left ventricle before sacrificing the mice.[18,47] After scaffolds were harvested, vasculature was visualized with multiphoton microscopy, and perfusion capacity was quantified by dissolving microspheres in xylene and measuring the fluorescence intensity with a plate reader (Tecan).[18,47] The phagocytic activity was measured with live cells on explanted scaffolds using the Vybrant Phagocytosis assay kit (Invitrogen) ($n = 4$).The background from scaffolds without fluorescent microangiography or phagocytosis assay was measured and subtracted from the values of test samples (12.34 for red fluorescence for perfusion capacity, 1.51 for green fluorescence for phagocytosis).

Statistical analysis

In all experiments, analytical results were expressed as means ± standard error of the mean. One-way analysis of variance was used to determine if statistical differences existed between groups. Comparisons of individual sample groups were performed using Tukey's range tests. For all experiments, $p < 0.05$ was considered statistically significant.

Results

Properties of collagen-filled, PEG-crosslinked poly(x% DTE-co-y% DT carbonate) scaffolds

To support cell growth and host tissue integration, a 3D scaffold requires features that facilitate the delivery of essential nutrients and oxygen to cells, as well as the removal of metabolic waste products generated by cells in the scaffold.[48] Therefore, poly(x% DTE-co-y% DT carbonate) polymers were crosslinked with PEG dihydrazide (Fig. 1A) in a salt bed, and following a salt-leaching procedure, the resulting scaffolds exhibited interconnected macroporous and microporous architecture to facilitate this nutrient and waste exchange (Fig. 1B).[25] To further encourage cell attachment, these synthetic scaffolds were filled with collagen, as evidenced by micro-CT (Fig. 1C).

The physical properties of the scaffold can be tuned by varying the concentration of the PEG dihydrazide crosslinker. Collagen-filled polymeric scaffolds containing 0–40 molar % PEG crosslinker were hydrated before measurement of wet modulus (Fig. 1D). In particular, scaffolds containing 0% or 40% crosslinker exhibited wet moduli of ≤10 kPa, and the highest modulus was measured for scaffolds containing 8% crosslinker (0.088 ± 0.01 MPa). These trends are likely due to increased water absorption into the scaffolds as the PEG content increases. PEG has also generally been shown to discourage nonspecific protein adsorption,[49] and as expected, the increased PEG content also correlated with the decreased fibrinogen deposition onto the scaffolds (Fig. 1E). Because collagen-filled polymeric scaffolds with 8% PEG exhibited mechanical properties similar to those of native soft tissue (~0.1 MPa),[50,51] as well as moderate levels of protein adsorption (~10 nm), this scaffold composition was used for subsequent biological experiments.

Controlled release of peptides from scaffolds

Scaffolds were loaded with either 75 μg of the pro-angiogenic peptide C16 or the anti-inflammatory peptide Ac-SDKP (Fig. 2A), or the combination of the two peptides (75 μg each peptide) (Fig. 2B). Cumulative release of these peptides into the surrounding medium was assessed by HPLC. Only slight differences were observed in the release profiles of scaffolds loaded with single type of peptides (Fig. 2A) or both types of peptides in combination (Fig. 2B). Despite significant differences in the sizes of these two peptides, both exhibited similar release profiles, with a burst release occurring within the first 3 days of the study period, resulting in a loss of ~40% of the total peptide content within each scaffold. This was followed by a little change in release up to the 14-day time point, when the study was concluded.

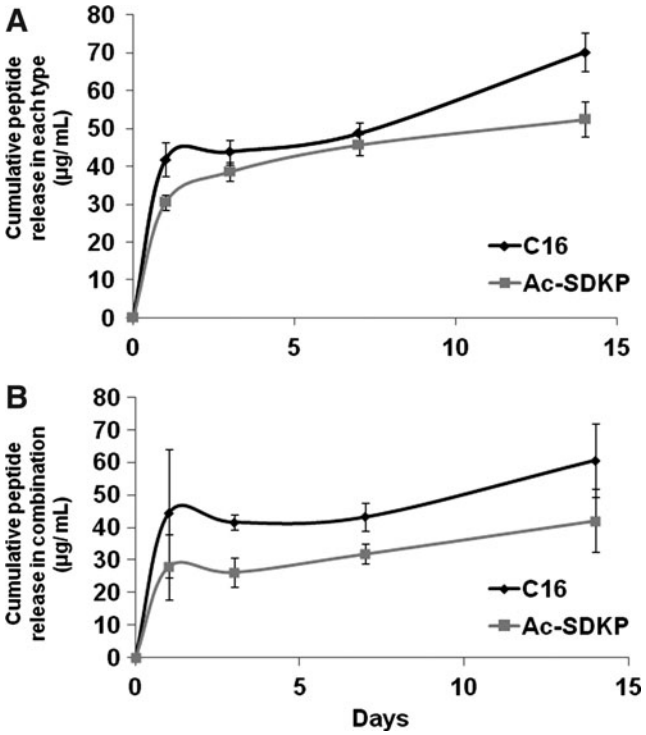

FIG. 2. Cumulative release of peptides from scaffolds. Collagen-filled scaffolds were loaded with 75 μg of either Ac-SDKP or C16 peptides **(A)**, or the combination of both peptides (75 μg each peptide) **(B)**. After gelation, phosphate-buffered saline (PBS) was added on top of the gel-filled scaffolds and left to incubate at 37°C until collected at either 1, 3, 7, or 14 days after gelation. PBS releasate samples were then analyzed by high-performance liquid chromatography to quantify the amount of released peptide, as determined by fitting to a standard curve ($n = 4$ per time point).

At this extended time point, the larger peptide (C16) exhibited a slightly elevated release from the scaffolds relative to a smaller peptide (Ac-SDKP). Subsequent biological experiments were conducted for 3–7 days to exploit the portion of the release curve, where the two peptides exhibit similar release kinetics.

Pro-angiogenic effect of C16 peptide on HUVEC migration and tubulogenesis within scaffolds

To validate the pro-angiogenic effects of the C16 peptide, HUVECs were seeded onto the top surface of collagen-filled scaffolds, with or without peptides embedded in the collagen gel. Within 72 h, scaffolds containing C16 exhibited enhanced migration of the HUVECs into the scaffold (Fig. 3A–C). In addition, the C16 peptide also enhanced the ability of HUVECs to form tubes as observed by confocal microscopy (Fig. 3D). At the highest dose of C16 employed (75 μg/scaffold), HUVECs formed 2.5-fold longer tubes than did HUVECs cultured in scaffolds in the absence of peptide. Therefore, in all further experiments, a dose of 75 μg/scaffold of C16 was used.

Anti-inflammatory effect of Ac-SDKP peptide on MDM activation

To characterize the dose-dependent anti-inflammatory effects of the Ac-SDKP peptide on MDMs, MDM phagocytosis of green fluorescent *E. coli* particles was used as a surrogate measure of inflammatory activity (Fig. 3E).[52] Strong phagocytic activity was detected in MDMs treated with the pro-inflammatory molecule LPS, but an opposite effect was observed in MDMs incubated with Ac-SDKP. Further, the phagocytic activity inversely correlated with the concentration of Ac-SDKP, suggesting that the peptide exerts anti-inflammatory effects on MDMs, which is consistent with previous observations by other groups.[53] Minimal phagocytosis was quantified at the 75 μg/scaffold dose of Ac-SDKP, and therefore, this dosage was used in all further experiments involving this peptide.

Elucidating interplay of inflammation and angiogenesis in vitro through MDM/HUVEC coculture studies

In light of the strong effects of C16 and Ac-SDKP on HUVEC-mediated tubulogenesis and macrophage activation, respectively, *in vitro* coculture studies were conducted involving both cell types on the scaffolds containing either or both of these peptides. In these studies, MDM phagocytosis (Fig. 4A) and HUVEC tubulogenesis (Fig. 4B) were visualized through the Vybrant phagocytosis assay kit (as described for the single-cell MDM experiments), and VCAM-1 staining, chosen as a marker of inflammatory-activated ECs to simultaneously verify the interactions between the MDMs and HUVECs and quantify tube formation.[41,42]

Both LPS and pro-angiogenic C16 treatment resulted in significant upregulation of phagocytic and tubulogenic activities, relative to untreated cocultures. These results were unexpected because previous evidence suggested that C16 suppresses leukocyte migration and activation.[54] Cocultures treated with anti-inflammatory Ac-SDKP exhibited decreased phagocytosis and tubulogenesis relative to untreated cocultures, which is notable given previous evidence showing that Ac-SDKP stimulates EC proliferation and tubulogenesis *in vitro*.[55,56] Interestingly, the inclusion of both peptides in the scaffolds led to divergent effects: the MDM phagocytic activity was comparable to levels following treatment with Ac-SDKP alone, whereas HUVEC tubulogenesis was similar to levels following treatment with C16 alone. Our results suggest that the scaffold system developed here enables independent control of inflammation and angiogenesis by decoupling interactions between the two cell types from exogenous stimuli provided through the synthetic substrate and peptides.

To provide potential mechanistic insight into this decoupled regulation, the levels of secreted pro-inflammatory cytokines (i.e., IL-1β, IL-6, IL-8, and TNF-α) were measured in the coculture supernatants (Fig. 5). Following treatment with C16, cytokine secretion increased significantly in comparison to untreated cocultures. However, treatment with Ac-SDKP resulted in decreased cytokine secretion. Co-delivery of both Ac-SDKP and C16 maintained a secretion profile similar to treatment with Ac-SDKP alone and significantly lower than the untreated cocultures. These results suggest that the reduced production of pro-inflammatory cytokines resulted in a reduction of phagocytic activity. However, due to the limited scope of cytokines measured, different cell signals might also involve the maintenance of

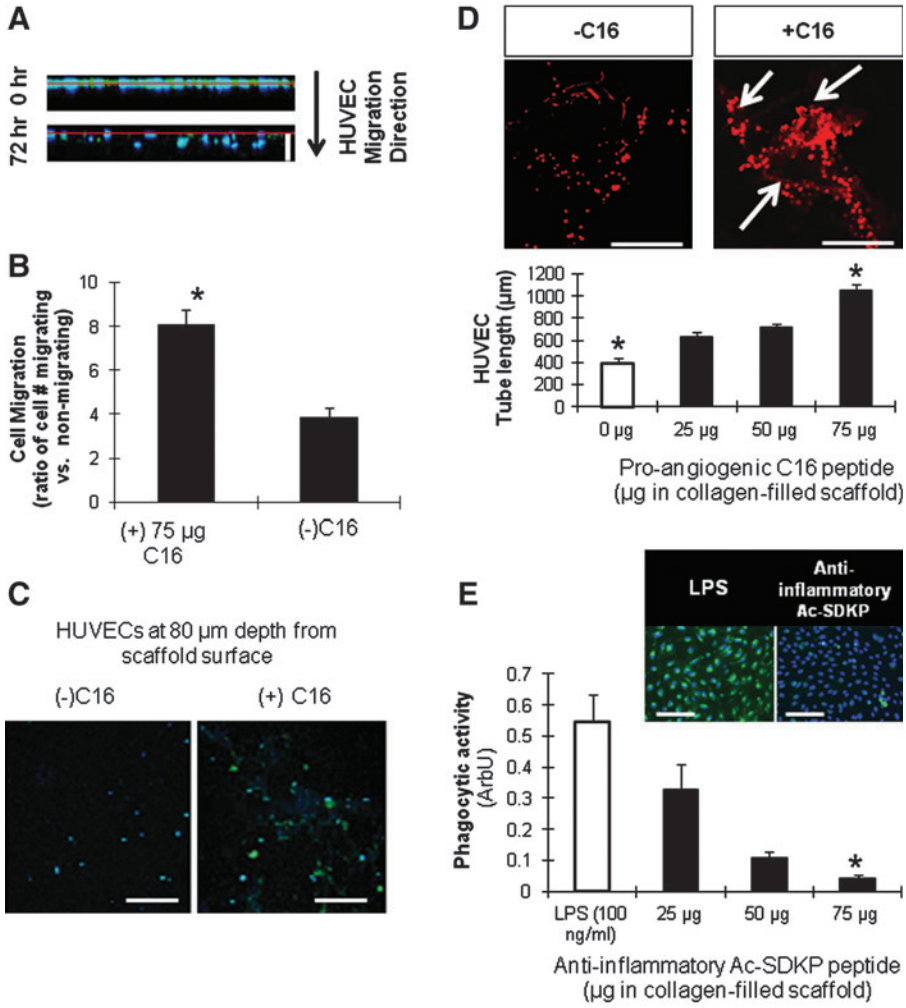

FIG. 3. Peptide characterization. **(A, B)** Human umbilical vein endothelial cell (HUVEC) migration into scaffolds. Cell nuclei (blue) and proliferating cells with BrdU incorporation (green). **(A)** Z-sectional projection of HUVEC migration from the surface (red line). White scale bar: 120 µm. **(B)** Effect of C16 peptide (75 µg/scaffold) on HUVEC migration at 72 h. Ratio of migrated versus nonmigrated HUVECs was defined as the number of cells migrated a distance >0 µm into the scaffolds divided by the number of cells remaining at the surface. **(C)** Representative images of HUVECs that have migrated 80 µm into the scaffold after 72 h. Scale bar: 100 µm. **(D)** Tubulogenesis (as measured by total tube length) of HUVECs around 40 µm into the scaffold in response to varying doses of pro-angiogenic C16 peptide. Ethidium bromide stained HUVECs with (right) and without (right) C16 shown in top images. White arrows indicate points of tube formation. Scale bar: 100 µm. **(E)** MDM phagocytic activity. Macrophages (blue) and phagocytized *Escherichia coli* particles (green) shown in the top images. The phagocytic activity presented by the green fluorescence intensity normalized to cell number in the bottom graph. Scale bar: 100 µm. **(B, D, E)** *$p < 0.05$ versus all the other conditions in same graph ($n = 5$). MDM, monocyte-derived macrophage. Color images available online at www.liebertpub.com/tea

high tubulogenic activity in the presence of both C16 and Ac-SDKP.

Angiogenesis and inflammatory activation in vivo *on collagen-filled scaffolds*

To determine if the *in vitro* results could be recapitulated *in vivo*, cell-free scaffolds were implanted subcutaneously into the dorsal regions of immunocompetent 129/SvEv mice for 7 days. At this time point, LPS-loaded scaffolds elicited a significant level of macrophage infiltration relative to unloaded scaffolds, as identified by $F4/80^+$ (a mouse macrophage marker) staining of frozen sections (Fig. 6A, B).[57] Macrophages were also visualized in high number in C16-loaded scaffolds. In contrast, the presence of Ac-SDKP significantly reduced the number of macrophages in the scaffold, and codelivery of C16 with Ac-SDKP did not recover the macrophage infiltration levels.

Tubulogenesis and macrophage activity were also quantified in the scaffolds indirectly by using measurements of perfusion capacity and phagocytosis, respectively (Fig. 6C–E). Consistent with measurements *in vitro*, C16 enhanced the blood vessel formation and macrophage activity on the scaffolds, while Ac-SDKP diminished both responses in comparison to the scaffolds without peptide loading. Codelivery of both peptides increased the blood vessel formation (Fig. 6D), while simultaneously decreasing macrophage activation compared to no peptide treatment (Fig. 6E). Therefore, these results verified *in vitro* observations in a more biologically complex, heterogeneous *in vivo* environment.

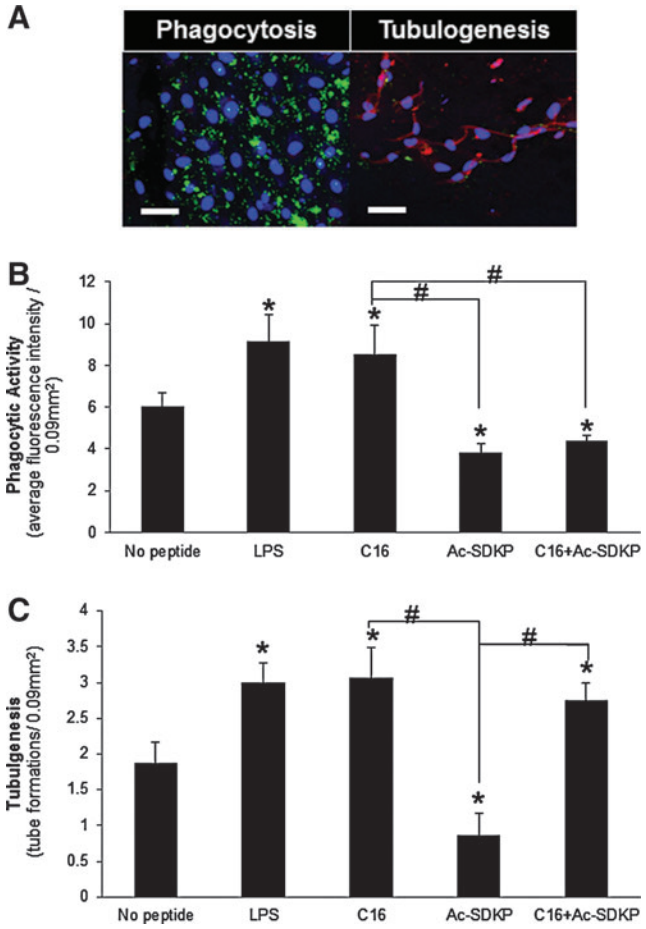

FIG. 4. *In vitro* coculture of MDMs and HUVECs in scaffolds. **(A)** Representative images of phagocytic macrophages (green, left) and HUVECs stained for vascular cell adhesion molecule-1 (VCAM-1) (red, right) as an indicator of inflammatory-stimulated tubulogenesis in C16 containing scaffolds. Scale bar: 50 μm. **(B)** Macrophage phagocytic activity as measured by average green fluorescence intensity per image field. **(C)** Tubulogenesis of HUVECs as measured by the number of tube formations per image field. **(B, C)** $^{*}p < 0.05$ compared to no peptide treatment; $^{\#}p < 0.05$ between groups connected by lines ($n = 8$). Color images available online at www.liebertpub.com/tea

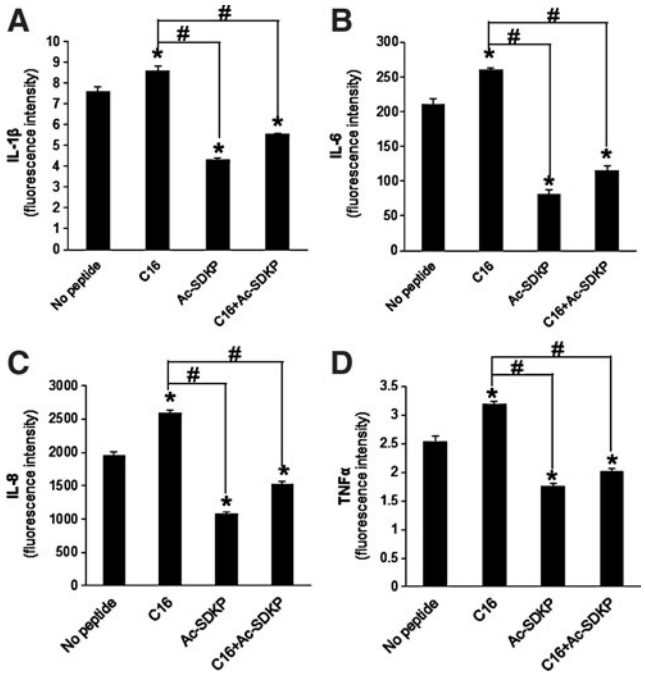

FIG. 5. Pro-inflammatory cytokine secretion. **(A)** Interleukin (IL)-1β, **(B)** IL-6, **(C)** IL-8, **(D)** tumor necrosis factor alpha (TNF-α) cytokine release from a coculture of HUVECs and MDMs in peptide-loaded scaffolds as measured by BD Cytometric Bead Array. $^{*}p < 0.05$ compared to no peptide treatment; $^{\#}p < 0.05$ between groups connected by lines ($n = 4$).

Discussion

Angiogenesis and inflammation are interdependent processes that unavoidably occur in response to implantation of biomaterial scaffolds. Several attempts have been made to reduce inflammation, while promoting angiogenesis to improve integration of scaffolds into host tissue, such as poly(lactic-co-glycolic acid) scaffolds implanted with a stromal-derived factor-1α-releasing pump[58] and injectable keratin biomaterials to promote cardiac tissue regeneration after myocardial infarction.[59] In the present study, a new method was developed for controlling the host response to biomaterial implants by simultaneously activating pro-angiogenic and anti-inflammatory responses using peptide-loaded, 3D synthetic scaffolds. This method is advantageous over previous methods that require a pump or release growth factors, which have unintended side effects.[19,20,26–29] The peptides used in this study stimulate little to no side effects as compared to growth factors and bioactive molecules that are commonly used,[19,20,26–29] further supporting their relevance for clinical applications.

Because inflammation and angiogenesis are highly interdependent, effective decoupling of their activities has been a staggering challenge to the fields of tissue engineering and regenerative medicine, and mechanistic insights into this relationship are undoubtedly needed for translation of novel therapies to the clinic. Through a series of *in vitro* and *in vivo* experiments employing bioactive peptides, the model system was shown here to actively control angiogenic and inflammatory activities in a user-specified manner, allowing for elucidation of novel aspects of this relationship and providing clues for further modulating the responses. Specifically, this study reveals a new method for promoting angiogenesis, while discouraging inflammation through simultaneous cotreatment with two peptides, pro-angiogenic C16 and anti-inflammatory Ac-SDKP, thereby providing a crucial step for improving tissue engineering strategies.

The tunable polymer scaffolds used in this study proved to be a useful platform for investigating soft tissues for several reasons: (1) scaffold mechanical properties were within the range of soft tissues that contact blood (~0.1 MPa), such as the vasculature and heart muscle,[50,51] (2) the level of protein adsorption to the scaffold facilitated cell attachment without causing over-accumulation of proteins,[31] and (3) pore interconnectivity promoted cell growth and migration into the scaffold, while maintaining efficient oxygen and nutrient transport.[60–63] The successful incorporation of

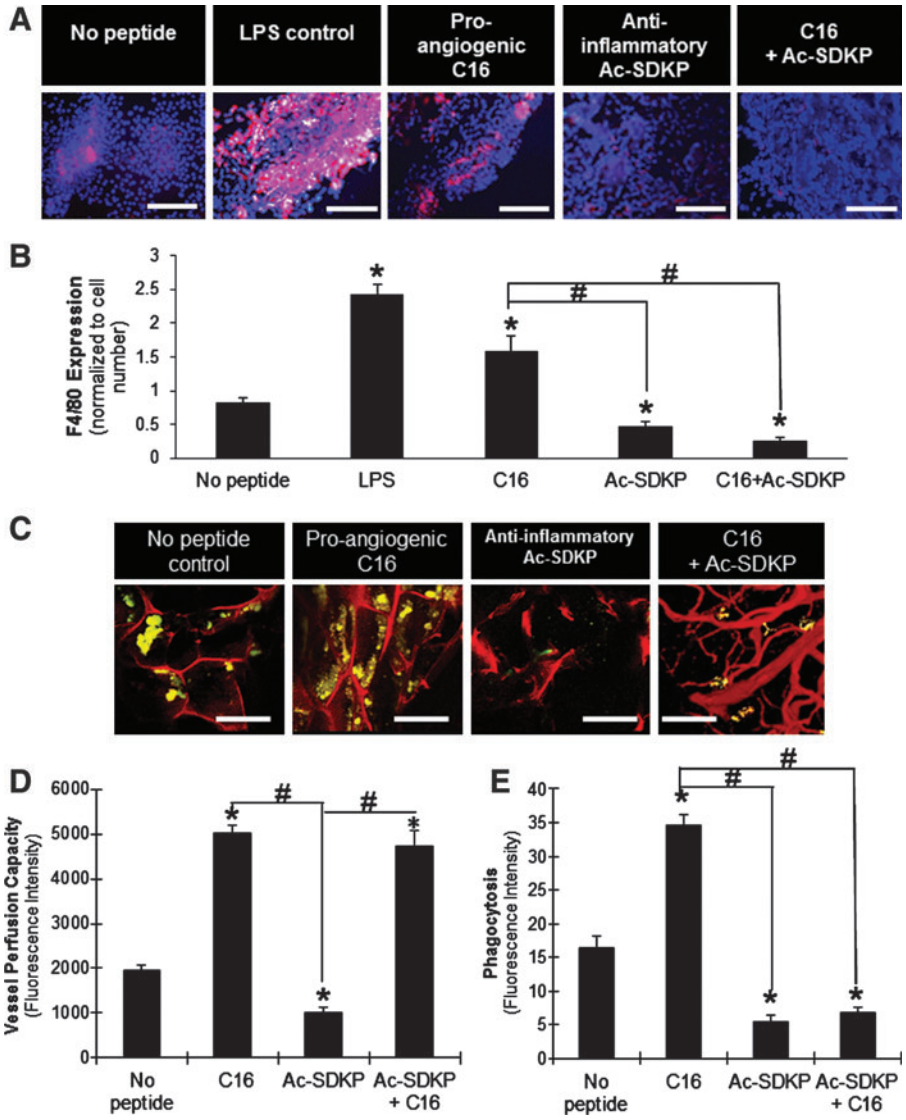

FIG. 6. *In vivo* implantation of scaffolds. **(A)** F4/80-positive macrophages (red) with cell nuclei (blue) infiltrated into implanted peptide-loaded scaffolds. Scale bar: 100 μm. **(B)** Quantification of F4/80 expression normalized to the corresponding cell number. **(C)** Blood vessel formation (red) visualized by fluorescent microangiography, and macrophages phagocytosing *E. coli* particles (yellow-green) in scaffold implants. Scale bar: 100 μm. **(D)** Vessel perfusion capacity as measured by red fluorescence intensity of perfused microspheres extracted from scaffolds. **(E)** Phagocytic activity (fluorescence intensity per image field). **(B, D, E)** $^{*}p < 0.05$ compared to no peptide treatment; $^{\#}p < 0.05$ between groups connected by lines ($n = 4$). Color images available online at www.liebertpub.com/tea

bioactive peptides into the scaffold, achieved via embedding in the collagen gel, provided a means for controlled peptide release. All *in vitro* tests were conducted with cell-seeded scaffolds for 3 days, which exposed the cultured cells to a burst release of peptides. All *in vivo* tests were conducted for 7 days which, according to the *in vitro* peptide release in Figure 2, likely exposed the host tissue to a similar amount of peptides as released over 3 days in *in vitro* studies. The longer, 7-day time point for *in vivo* experiments was chosen to allow for substantial cell infiltration, in accordance with previous studies that have shown blood vessel ingrowth into implanted scaffolds at 7 days postimplantation.[17,18]

Previous studies with laminin-derived peptides, such as pro-angiogenic C16, revealed increased EC attachment, aortic ring sprouting, and melanoma cell migration.[26,30,64] The present study demonstrated that the angiogenic activities of HUVECs were dependent upon the dose of C16 peptide (Fig. 3B–D), and that the phagocytic activities of MDMs correlated inversely with the dose of anti-inflammatory Ac-SDKP peptide (Fig. 3E). The use of these two peptides, as well as the pro-inflammatory molecule LPS, revealed a high degree of interdependence between angiogenesis and inflammation in the coculture system. For example, LPS stimulated the phagocytic activity of the MDMs as well as the tubulogenic activity of HUVECs (Fig. 4B, C), indicating a pro-angiogenic response to the inflammatory stimulus. Similarly, pro-angiogenic C16 stimulated not only the EC tube formation, but also MDM phagocytosis, both of which were comparable to pro-inflammatory LPS treatment, indicating that angiogenic stimulation also influences inflammation. Conversely, anti-inflammatory Ac-SDKP decreased both EC tube formation and MDM phagocytosis (Fig. 4B, C). These results explain why pro-angiogenic therapies alone often promote unintentional inflammatory activation.[15–18,65,66] Interestingly, simultaneous cotreatment with the two peptides activated angiogenesis, but suppressed the inflammatory response both *in vitro* (Fig. 4) and *in vivo* (Fig. 6), suggesting a potential solution to decoupling inflammation and angiogenesis.

In addition to monitoring tubulogenic and phagocytic activities, the secretion of cytokines by macrophages in the *in vitro* coculture was measured to elucidate the role of macrophages in modulating angiogenesis and inflammation

(Fig. 5). During the foreign body response, macrophages secrete IL-1β, IL-6, IL-8, and TNF-α to recruit additional macrophages to the implant site and aid in the degradation of foreign material.[6,67,68] Secretion of pro-inflammatory cytokines followed a profile similar to that of phagocytic activity *in vitro* (Fig. 4) and F4/80 expression *in vivo* (Fig. 6). Specifically, treatment with the pro-angiogenic C16 peptide stimulated an increase in cytokine secretion relative to control, but anti-inflammatory Ac-SDKP treatment diminished this response, and simultaneous cotreatment with the two peptides did not statistically change the cytokine levels as compared to Ac-SDKP treatment alone (Fig. 5). The low levels of pro-inflammatory cytokines as observed from the cotreatment might direct a mechanism to reduce inflammatory responses, while maintaining pro-angiogenic responses. *In vivo* experiments confirmed the trends found from the *in vitro* experiments in terms of angiogenic and inflammatory activities with the use of functional peptides, and verified that the cotreatment of pro-angiogenic and anti-inflammatory peptides optimized host responses by increasing angiogenesis, while decreasing inflammation.

Conclusions

Clinically relevant tissue engineering strategies require angiogenesis at the site of implantation to enhance integration of scaffolds with host tissue and desire a reduction of the inflammatory response to expedite healing time. This study employed a model 3D scaffold system with embedded peptides to reveal the interdependence of these two processes as well as establishing that angiogenesis can be promoted, while strongly discouraging macrophage infiltration *in vivo* through simultaneous cotreatment with pro-angiogenic C16 and anti-inflammatory Ac-SDKP peptides. This finding has strong implications for developing novel therapies that aim to effectively control these responses through relatively simple techniques. Several studies have investigated the unintentional inflammatory response that coincides with pro-angiogenic therapies[15–18,65,66] and this study suggests a potential means for regulating these responses. The dual peptide delivery system used here provides a potential means to optimize the host responses in a user-specified manner for regeneration of soft tissues.

Acknowledgments

The authors acknowledge Aidan R.W. Boone for his assistance in experimenting, the Vanderbilt Institute of Nanoscale Science and Engineering (VINSE) for SEM imaging, Jason Tucker-Swartz, Dr. Melissa Skala for OCT imaging, Dr. Hynda K. Kleinman (NIH) for her helpful discussions, the Vanderbilt University School of Medicine (VUMC) Cell Imaging Shared Resource for confocal imaging, and Will Stokes and Dr. Xintong Wang for HPLC measurement. This study was supported by NIH HL091465 and NSF 1006558. SSY and TDG acknowledge support from a grant from the Department of Defense Congressionally Directed Medical Research Programs #W81XWH-10–1-0684. VINSE is housed in facilities renovated under NSF ARI-R2 DMR-0963361.

Disclosure Statement

No competing financial interests exist.

References

1. Bailey, L.O., Washburn, N.R., Simon, C.G., Chan, E.S., and Wang, F.W. Quantification of inflammatory cellular responses using real-time polymerase chain reaction. J Biomed Mater Res A **69A,** 305, 2004.
2. Hu, W.J., Eaton, J.W., and Tang, L.P. Molecular basis of biomaterial-mediated foreign body reactions. Blood **98,** 1231, 2001.
3. Ratner, B.D., Gladhill, K.W., and Horbett, T.A. Analysis of *in vitro* enzymatic and oxidative degradation of polyurethanes. J Biomed Mater Res **22,** 509, 1988.
4. Silva, M.M., Cyster, L.A., Barry, J.J., Yang, X.B., Oreffo, R.O., Grant, D.M., *et al.* The effect of anisotropic architecture on cell and tissue infiltration into tissue engineering scaffolds. Biomaterials **27,** 5909, 2006.
5. Robbins, C.S., and Swirski, F.K. The multiple roles of monocyte subsets in steady state and inflammation. Cell Mol Life Sci **67,** 2685, 2010.
6. Ariganello, M.B., Simionescu, D.T., Labow, R.S., and Lee, J.M. Macrophage differentiation and polarization on a decellularized pericardial biomaterial. Biomaterials **32,** 439, 2011.
7. Murray, P.J., and Wynn, T.A. Obstacles and opportunities for understanding macrophage polarization. J Leukoc Biol **89,** 557, 2011.
8. Lutolf, M.P., and Hubbell, J.A. Synthetic biomaterials as instructive extracellular microenvironments for morphogenesis in tissue engineering. Nat Biotechnol **23,** 47, 2005.
9. Szekanecz, Z., and Koch, A.E. Mechanisms of disease: angiogenesis in inflammatory diseases. Nat Clin Pract Rheumatol **3,** 635, 2007.
10. Cotran, R.S., and Pober, J.S. Cytokine-endothelial interactions in inflammation, immunity, and vascular injury. J Am Soc Nephrol **1,** 225, 1990.
11. Imhof, B.A., and Aurrand-Lions, M. Angiogenesis and inflammation face off. Nat Med **12,** 171, 2006.
12. Costa, C., Incio, J., and Soares, R. Angiogenesis and chronic inflammation: cause or consequence? Angiogenesis **10,** 149, 2007.
13. Shamamian, P., Schwartz, J.D., Pocock, B.J., Monea, S., Whiting, D., Marcus, S.G., *et al.* Activation of progelatinase A (MMP-2) by neutrophil elastase, cathepsin G, and proteinase-3: a role for inflammatory cells in tumor invasion and angiogenesis. J Cell Physiol **189,** 197, 2001.
14. Lee, S., Zheng, M., Kim, B., and Rouse, B.T. Role of matrix metalloproteinase-9 in angiogenesis caused by ocular infection with herpes simplex virus. J Clin Invest **110,** 1105, 2002.
15. Webb, N.J., Myers, C.R., Watson, C.J., Bottomley, M.J., and Brenchley, P.E. Activated human neutrophils express vascular endothelial growth factor (VEGF). Cytokine **10,** 254, 1998.
16. Scapini, P., Nesi, L., Morini, M., Tanghetti, E., Belleri, M., Noonan, D., *et al.* Generation of biologically active angiostatin kringle 1–3 by activated human neutrophils. J Immunol **168,** 5798, 2002.
17. Sung, H.J., Meredith, C., Johnson, C., and Galis, Z.S. The effect of scaffold degradation rate on three-dimensional cell growth and angiogenesis. Biomaterials **25,** 5735, 2004.
18. Sung, H.J., Johnson, C.E., Lessner, S.M., Magid, R., Drury, D.N., and Galis, Z.S. Matrix metalloproteinase 9 facilitates collagen remodeling and angiogenesis for vascular constructs. Tissue Eng **11,** 267, 2005.
19. Yang, F., Yang, X.P., Liu, Y.H., Xu, J., Cingolani, O., Rhaleb, N.E., *et al.* Ac-SDKP reverses inflammation and fibrosis in

rats with heart failure after myocardial infarction. Hypertension **43,** 229, 2004.
20. Rasoul, S., Carretero, O.A., Peng, H.M., Cavasin, M.A., Zhuo, J.L., Sanchez-Mendoza, A., *et al.* Antifibrotic effect of Ac-SDKP and angiotensin-converting enzyme inhibition in hypertension. J Hypertens **22,** 593, 2004.
21. Alexandru, N., Popov, D., and Georgescu, A. Platelet dysfunction in vascular pathologies and how can it be treated. Thromb Res **129,** 116, 2011.
22. Fleiner, M., Kummer, M., Mirlacher, M., Sauter, G., Cathomas, G., Krapf, R., *et al.* Arterial neovascularization and inflammation in vulnerable patients - Early and late signs of symptomatic atherosclerosis. Circulation **110,** 2843, 2004.
23. Yu, C., and Kohn, J. Tyrosine-PEG-derived poly(ether carbonate)s as new biomaterials. Part I: synthesis and evaluation. Biomaterials **20,** 253, 1999.
24. Magno, M.H.R., Kim, J., Srinivasan, A., McBride, S., Bolikal, D., Darr, A., *et al.* Synthesis, degradation and biocompatibility of tyrosine-derived polycarbonate scaffolds. J Mater Chem **20,** 8885, 2010.
25. Sung, H.J., Labazzo, K.M.S., Bolikal, D., Weiner, M.J., Zimnisky, R., and Kohn, J. Angiogenic competency of biodegradable hydrogels fabricated from polyethylene glycol-crosslinked tyrosine-derived polycarbonates. Eur Cells Mater **15,** 77, 2008.
26. Ponce, M.L., Hibino, S., Lebioda, A.M., Mochizuki, M., Nomizu, M., and Kleinman,H.K. Identification of a potent peptide antagonist to an active laminin-1 sequence that blocks angiogenesis and tumor growth. Cancer Res **63,** 5060, 2003.
27. Malinda, K.M., Nomizu, M., Chung, M., Delgado, M., Kuratomi, Y., Yamada, Y., *et al.* Identification of laminin alpha1 and beta1 chain peptides active for endothelial cell adhesion, tube formation, and aortic sprouting. FASEB J **13,** 53, 1999.
28. Cavasin, M.A. Therapeutic potential of thymosin-beta4 and its derivative N-acetyl-seryl-aspartyl-lysyl-proline (Ac-SDKP) in cardiac healing after infarction. Am J Cardiovasc Drugs **6,** 305, 2006.
29. Cingolani, O.H., Yang, X.P., Liu, Y.H., Villanueva, M., Rhaleb, N.E., and Carretero, O.A. Reduction of cardiac fibrosis decreases systolic performance without affecting diastolic function in hypertensive rats. Hypertension **43,** 1067, 2004.
30. Kuratomi, Y., Nomizu, M., Tanaka, K., Ponce, M.L., Komiyama, S., Kleinman, H.K., *et al.* Laminin gamma 1 chain peptide, C-16 (KAFDITYVRLKF), promotes migration, MMP-9 secretion, and pulmonary metastasis of B16-F10 mouse melanoma cells. Br J Cancer **86,** 1169, 2002.
31. Sung, H.J., Luk, A., Murthy, N.S., Liu, E., Jois, M., Joy, A., *et al.* Poly(ethylene glycol) as a sensitive regulator of cell survival fate on polymeric biomaterials: the interplay of cell adhesion and pro-oxidant signaling mechanisms. Soft Matter **6,** 5196, 2010.
32. Kitamura, N., Nishinarita, S., Takizawa, T., Tomita, Y., and Horie, T. Cultured human monocytes secrete fibronectin in response to activation by proinflammatory cytokines. Clin Exp Immunol **120,** 66, 2000.
33. Clark, R.A., Folkvord, J.M., and Nielsen, L.D. Either exogenous or endogenous fibronectin can promote adherence of human endothelial cells. J Cell Sci **82,** 263, 1986.
34. Voinova, M.V., Rodahl, M., Jonson, M., and Kasemo, B. Viscoelastic acoustic response of layered polymer films at fluid-solid interfaces: continuum mechanics approach. Phys Scripta **59,** 391, 1999.
35. Weber, N., Pesnell, A., Bolikal, D., Zeltinger, J., and Kohn, J. Viscoelastic properties of fibrinogen adsorbed to the surface of biomaterials used in blood-contacting medical devices. Langmuir **23,** 3298, 2007.
36. Sung, H.J., Yee, A., Eskin, S.G., and McIntire, L.V. Cyclic strain and motion control produce opposite oxidative responses in two human endothelial cell types. Am J Physiol Cell Ph **293,** C87, 2007.
37. Nau, G.J., Richmond, J.F., Schlesinger, A., Jennings, E.G., Lander, E.S., and Young, R.A. Human macrophage activation programs induced by bacterial pathogens. Proc Natl Acad Sci U S A **99,** 1503, 2002.
38. Volkov, L., Quere, P., Coudert, F., Comte, L., Antipov, Y., and Praloran, V. The tetrapeptide AcSDKP, a negative regulator of cell cycle entry, inhibits the proliferation of human and chicken lymphocytes. Cell Immunol **168,** 302, 1996.
39. Foukas, L.C., Katsoulas, H.L., Paraskevopoulou, N., Metheniti, A., Lambropoulou, M., and Marmaras, V.J. Phagocytosis of *Escherichia coli* by insect hemocytes requires both activation of the Ras/mitogen-activated protein kinase signal transduction pathway for attachment and beta3 integrin for internalization. J Biol Chem **273,** 14813, 1998.
40. Wan, C.P., Park, C.S., and Lau, B.H. A rapid and simple microfluorometric phagocytosis assay. J Immunol Methods **162,** 1, 1993.
41. Chen, A., Dong, L., Leffler, N.R., Asch, A.S., Witte, O.N., and Yang, L.V. Activation of GPR4 by acidosis increases endothelial cell adhesion through the camp/epac pathway. PLoS One **6,** e27586, 2011.
42. Xue, Y., Liu, X., and Sun, J. PU/PTFE-stimulated monocyte-derived soluble factors induced inflammatory activation in endothelial cells. Toxicol *In Vitro* **24,** 404, 2010.
43. Liu, J.M., Lawrence, F., Kovacevic, M., Bignon, J., Papadimitriou, E., Lallemand, J.Y., *et al.* The tetrapeptide AcSDKP, an inhibitor of primitive hematopoietic cell proliferation, induces angiogenesis *in vitro* and *in vivo*. Blood **101,** 3014, 2003.
44. Mantovani, A., Sozzani, S., Locati, M., Allavena, P., and Sica, A. Macrophage polarization: tumor-associated macrophages as a paradigm for polarized M2 mononuclear phagocytes. Trends Immunol **23,** 549, 2002.
45. Propst, K.L., Mima, T., Choi, K.H., Dow, S.W., and Schweizer, H.P. A Burkholderia pseudomallei deltapurM mutant is avirulent in immunocompetent and immunodeficient animals: candidate strain for exclusion from select-agent lists. Infect Immun **78,** 3136, 2010.
46. Dace, D.S., Khan, A.A., Kelly, J., and Apte, R.S. Interleukin-10 promotes pathological angiogenesis by regulating macrophage response to hypoxia during development. PLoS One **3,** e3381, 2008.
47. Johnson, C., Sung, H.J., Lessner, S.M., Fini, M.E., and Galis, Z.S. Matrix metalloproteinase-9 is required for adequate angiogenic revascularization of ischemic tissues - potential role in capillary branching. Circ Res **94,** 262, 2004.
48. Cuchiara, M.P., Allen, A.C., Chen, T.M., Miller, J.S., and West, J.L. Multilayer microfluidic PEGDA hydrogels. Biomaterials **31,** 5491, 2010.
49. Prime, K.L., and Whitesides, G.M. Self-assembled organic monolayers: model systems for studying adsorption of proteins at surfaces. Science **252,** 1164, 1991.
50. Choi, A., and Zheng, Y. Estimation of Young's modulus and Poisson's ratio of soft tissue from indentation using two different-sized indentors: finite element analysis of the finite deformation effect. Med Biol Eng Comput **43,** 258, 2005.

51. McKee, C.T., Last, J.A., Russell. P., and Murphy, C.J. Indentation versus tensile measurements of Young's modulus for soft biological tissues. Tissue Eng Part B Rev **17,** 155, 2011.
52. Bianco, C., Griffin, F.M., and Silverstein, S.C. Studies of the macrophage complement receptor. Alteration of receptor function upon macrophage activation. J Exp Med **141,** 1278, 1975.
53. Sharma, U., Rhaleb, N.E., Pokharel, S., Harding, P., Rasoul, S., Peng, H., *et al.* Novel anti-inflammatory mechanisms of N-Acetyl-Ser-Asp-Lys-Pro in hypertension-induced target organ damage. Am J Physiol Heart Circ Physiol **294,** H1226, 2008.
54. Han, S., Arnold, S.A., Sithu, S.D., Mahoney, E.T., Geralds, J.T., Tran, P., *et al.* Rescuing vasculature with intravenous angiopoietin-1 and αvβ3 integrin peptide is protective after spinal cord injury. Brain **133,** 1026, 2010.
55. Sosne, G., Qiu, P., Goldstein, A.L., and Wheater, M. Biological activities ofthymosin β4 defined by active sites in short peptide sequences. FASEB J **24,** 2144, 2010.
56. Waeckel, L., Bignon, J., Liu, J.M., Markovits, D., Ebrahimian, T.G., Vilar, J., *et al.* Tetrapeptide acsdkp induces postischemic neovascularization through monocyte chemoattractant protein-1 signaling. Arterioscler Thromb Vasc Biol **26,** 773, 2006.
57. Austyn, J.M., and Gordon, S. F4-80, a monoclonal-antibody directed specifically against the mouse macrophage. Eur J Immunol **11,** 805, 1981.
58. Thevenot, P.T., Nair, A.M., Shen, J., Lotfi, P., Ko, C.Y., and Tang, L. The effect of incorporation of SDF-1alpha into PLGA scaffolds on stem cell recruitment and the inflammatory response. Biomaterials **31,** 3997, 2010.
59. Shen, D., Wang, X., Zhang, L., Zhao, X., Li, J., Cheng, K., *et al.* The amelioration of cardiac dysfunction after myocardial infarction by the injection of keratin biomaterials derived from human hair. Biomaterials **32,** 9290, 2011.
60. Ring, A., Goertz, O., Steinstraesser, L., Kuhnen, C., Schmitz, I., Muhr, G., *et al.* Analysis of biodegradation of copolymer dermis substitutes in the dorsal skinfold chamber of balb/c mice. Eur J Med Res **11,** 471, 2006.
61. Druecke, D., Langer, S., Lamme, E., Pieper, J., Ugarkovic, M., Steinau, H.U., *et al.* Neovascularization of poly(ether ester) block-copolymer scaffolds *in vivo*: Long-term investigations using intravital fluorescent microscopy. J Biomed Mater Res A **68A,** 10, 2004.
62. Sieminski, A.L., and Gooch, K.J. Biomaterial-microvasculature interactions. Biomaterials **21,** 2233, 2000.
63. Dziubla, T.D., and Lowman, A.M. Vascularization of PEG-grafted macroporous hydrogel sponges: A three-dimensional *in vitro* angiogenesis model using human microvascular endothelial cells. J Biomed Mater Res A **68A,** 603, 2004.
64. Ponce, M.L., Nomizu, M., and Kleinman, H.K. An angiogenic laminin site and its antagonist bind through the alpha(v)beta3 and alpha5beta1 integrins. Faseb J **15,** 1389, 2001.
65. Madden, L.R., Mortisen, D.J., Sussman, E.M., Dupras, S.K., Fugate, J.A., Cuy, J.L., *et al.* Proangiogenic scaffolds as functional templates for cardiac tissue engineering. Proc Natl Acad Sci U S A **107,** 15211, 2010.
66. Barker, T.H., Framson, P., Puolakkainen, P.A., Reed, M., Funk, S.E., and Sage, E.H. Matricellular homologs in the foreign body response - Hevin suppresses inflammation, but Hevin and SPARC together diminish angiogenesis. Am J Pathol **166,** 923, 2005.
67. Anderson, J.M., Rodriguez, A., and Chang, D.T. Foreign body reaction to biomaterials. Semin Immunol **20,** 86, 2008.
68. Ainslie, K.M., Tao, S.L., Popat, K.C., Daniels, H., Hardev, V., Grimes, C.A., *et al. In vitro* inflammatory response of nanostructured titania, silicon oxide, and polycaprolactone. J Biomed Mater Res A **91A,** 647, 2009.

Address correspondence to:
Hak-Joon Sung, PhD
Department of Biomedical Engineering
Vanderbilt University
VU Station B #351631
2301 Vanderbilt Place
Nashville, TN 37235

E-mail: hak-joon.sung@vanderbilt.edu

Received: March 8, 2012
Accepted: August 24, 2012
Online Publication Date: October 18, 2012